Rhythmicity facilitates pitch discrimination: Differential roles of low and high frequency neural oscillations

Andrew Chang [a], Dan J. Bosnyak [a,b], Laurel J. Trainor [a,b,c,*]

[a] Department of Psychology, Neuroscience and Behaviour, McMaster University, Hamilton, ON L8S 4K1, Canada
[b] McMaster Institute for Music and the Mind, McMaster University, Hamilton, ON L8S 4K1, Canada
[c] Rotman Research Institute, Baycrest Hospital, Toronto, ON M6A 2E1, Canada

ARTICLE INFO

ABSTRACT

Previous studies indicate that temporal predictability can enhance timing and intensity perception, but it is not known whether it also enhances pitch perception, despite pitch being a fundamental perceptual attribute of sound. Here we investigate this in the context of rhythmic regularity, a form of predictable temporal structure common in sound streams, including music and speech. It is known that neural oscillations in low (delta: 1–3 Hz) and high (beta: 15–25 Hz) frequency bands entrain to rhythms in phase and power, respectively, but it is not clear why both low and high frequency bands entrain to external rhythms, and whether they and their coupling serve different perceptual functions. Participants discriminated near-threshold pitch deviations (targets) embedded in either rhythmic (regular/isochronous) or arrhythmic (irregular/non-isochronous) tone sequences. Psychophysically, we found superior pitch discrimination performance for target tones in rhythmic compared to arrhythmic sequences. Electroencephalography recordings from auditory cortex showed that delta phase, beta power modulation, and delta-beta coupling were all modulated by rhythmic regularity. Importantly, trial-by-trial neural-behavioural correlational analyses showed that, prior to a target, the depth of U-shaped beta power modulation predicted pitch discrimination sensitivity whereas cross-frequency coupling strength predicted reaction time. These novel findings suggest that delta phase might reflect rhythmic temporal expectation, beta power temporal attention, and delta-beta coupling auditory-motor communication. Together, low and high frequency auditory neural oscillations reflect different perceptual functions that work in concert for tracking rhythmic regularity and proactively facilitate pitch perception.

1. Introduction

Predictive temporal structure is essential across many aspects of human cognition and behaviour, ranging from proactively optimizing perceptual processing (Haegens and Zion Golumbic, 2018) and speech communication (Giraud and Poeppel, 2012) to facilitating interpersonal coordination (Chang et al., 2017, 2019; Savage et al., 2015) and prosocial behaviours (Cirelli et al., 2014, 2018). Rhythm is a form of predictable temporal structure, in which events tend to occur at regular time intervals or have recurring characteristics (Nobre and van Ede, 2018). Given that speech and music unfold over time, and sound events are fleeting, it is perhaps not surprising that speech and music are temporally structured (Ding et al., 2017) as the resulting rhythmic regularity (musical beat; syllable timing) enables prediction of when important upcoming information is likely to occur. In the present paper we

manipulate rhythmic predictability to investigate whether temporal predictability enhances pitch perception.

Sounds can vary over time in multiple aspects. The temporal aspect involves variations in sound onsets, durations and rhythm; the intensity aspect involves variations in sound pressure; and the spectral aspect involves variations in frequency (e.g., resulting in pitch changes). Previous studies show that rhythmic regularity in auditory sequences facilitates detection of near-threshold timing and intensity deviations (e.g., Henry and Herrmann, 2014; McAuley and Fromboluti, 2014). However, to our knowledge, none have investigated the effect of rhythmic regularity on detecting near-threshold pitch changes, despite pitch being a fundamental perceptual attribute of sound crucial for speech, music and object identification. It is not obvious a priori that rhythmic regularity would enhance pitch perception similarly to how it enhances time and intensity perception because pitch perception can be dissociated from time and

intensity perception. For example, people with amusia or tone deafness typically have auditory perceptual deficits in the spectral domain but not in the temporal or intensity domains (Peretz, 2016; Zendel et al., 2015). Therefore, it is important to investigate whether rhythmicity facilitates near-threshold pitch discrimination in order to determine whether rhythmicity enhances all of the major dimensions of auditory perception.

Neural oscillations in the brain synchronize their activity to rhythmic regularities in sensory input, which has been termed "neural entrainment", and this is regarded as an important neural mechanism for tracking rhythmicity (Haegens and Zion Golumbic, 2018). In monkeys, electrophysiological recordings showed that the phase of low frequency oscillations (delta band: 1–3 Hz) time-lock and entrain to external rhythmic sensory input (Lakatos et al., 2013, 2016), and sensory input coincident with the excitatory phase is selectively facilitated (Schroeder and Lakatos, 2009; Calderone et al., 2014). In humans, electroencephalography (EEG) and magnetoencephalography (MEG) studies show that fidelity of delta phase entrainment associates with perceptual facilitation in the auditory temporal and intensity domains (e.g., Arnal et al., 2015; Bauer et al., 2018; Henry and Obleser, 2012; Henry et al., 2014; ten Oever et al., 2017), but it remains uncertain whether delta phase associates with facilitated pitch perception. Again, rhythmic facilitation might operate differently at the neural oscillatory level for perceiving pitch changes compared to temporal and intensity changes. Therefore, it is important to investigate whether delta phase associates with perceptual facilitation in the spectral domain as it does in the temporal and intensity domains.

Power modulations in high frequency oscillations (beta band: 15–25 Hz) also entrain to rhythmic regularity and reflect temporal prediction, but perceptual consequences have not been investigated. In response to a rhythmic tone sequence, beta power decreases following each tone onset, and then increases with the appropriate slope to anticipate the predicted onset time of the upcoming tone, dependent on sequence tempo (Fujioka et al., 2012; Cirelli et al., 2014). Beta modulation is disrupted in non-rhythmic sequences (Fujioka et al., 2009, 2012) and modulated by hierarchical timing structures (e.g., waltz, march) (Snyder and Large, 2005; Iversen et al., 2009; Fujioka et al., 2015). Beyond time, a few previous studies hinted at the role of beta in prediction of pitch (Chang et al., 2016, 2018; Sedley et al., 2016); however, perceptual performance was not measured or related to beta oscillations in these studies. Here we hypothesized that the magnitude of beta power entrainment in a rhythmic context associates with increased pitch sensitivity.

A fundamental question concerns why delta phase and beta power both entrain to external rhythms. Do they implement different perceptual functions? One MEG study showed pre-target delta phase, beta power, and delta-beta coupling all predict detection of a timing deviation (Arnal et al., 2015), but did not differentiate them functionally. Another MEG study suggested delta and beta entrainments represent opposite directions of auditory-motor communication (Morillon and Baillet, 2017), but how they differ in perceptual functions remained unclear.

The current study investigates (1) whether rhythmic regularity facilitates near-threshold pitch discrimination and (2) how neural oscillations associate with such facilitation. Participants performed a pitch discrimination task embedded in either rhythmic (regular, isochronous) or arrhythmic (irregular, non-isochronous) tone sequences. Behaviourally, we hypothesized that rhythmic regularity would facilitate pitch discrimination sensitivity and reaction time. Neurally, we focused on the oscillatory signals generated from bilateral auditory cortices, as they are regarded to be the major sources of auditory neural entrainment activities (Fujioka et al., 2012; Morillon and Baillet, 2017) and the primary regions for processing pitch (McDermott, 2018). Specifically, we used dipole models as spatial filters to extract the source waveforms that focused on activity in auditory cortices. We hypothesized that rhythmicity would modulate oscillatory activities, including not only the phase of low-frequency oscillatory activity, but beta power and delta-beta coupling as well. Further, we explored how pre-target delta phase, beta

power modulation and delta-beta coupling would predict different aspects of perceptual performance at a trial-by-trial level.

2. Materials and methods

2.1. Participants

The 16 participants (18–27 years old, mean age 19.3 ± 2.3, 11 females) were students at McMaster University and received course credit for completing the study. Participants were screened by a self-report survey to ensure they had normal hearing, were neurologically healthy and were right-handed. Signed informed consent was obtained from each participant. The McMaster University Research Ethics Board approved all procedures.

2.2. Stimuli

Auditory stimuli were computer-generated complex tones. Each tone was composed by summing sinusoidal waves at the fundamental frequency (F0) and two overtones (F1 and F2) with slope -6 dB/oct and frequency components added in random phases. Tones had 10 ms rise and fall times and a 40 ms steady-state duration. Sounds were presented at 60.6 dB SPL (C weighted), measured through an artificial ear (type 4152, Brüel & Kjær) with a sound level meter (type 2270, Brüel & Kjær). All stimulus sequences were presented under the control of a digital signal processor (Tucker Davis RP2.1) and delivered binaurally via ear inserts (Etymotic Research ER-2).

2.3. Procedure

Initially, a calibration session was conducted to estimate individual pitch discrimination thresholds in order to present near-threshold stimuli for each participant in the main experiment. We used a 2-alternative forced-choice procedure. On each trial, participants heard a standard tone (F0 fixed at 500 Hz) and a target tone (8.4 dB louder than the standard tone, as presented during the main experiment) that was either higher or lower in pitch (random presentation order), with a 500 ms inter-onset interval (IOI). Participants were required to judge which tone was higher in pitch by pressing one of two buttons. The target tone started at $500 * e^{\pm 0.02}$ Hz ($\approx$510.1 and 490.1 Hz), and the 1-up/2-down procedure adjusted the F0 of the target tone according to the performance on previous trials (Levitt, 1971), with step size $e^{0.002}$ ($\approx$1 Hz). Over 40 trials, the 70.7% correct pitch discrimination thresholds were estimated for target tones higher and lower than the standard tone. The logarithmic midpoint between these two thresholds (one higher and one lower than 500 Hz) was the point of subjective equality (PSE), and the just-noticeable difference (Δ) was the logarithmic distance between the PSE and a threshold. This calibration session took 5–10 min. The mean estimated PSE was 498.07 ± 0.45 Hz and the estimated Δ was 3.69 ± 0.40 Hz across participants (mean $\pm$ standard error).

To manipulate rhythmic regularity (Rhythmicity), the experiment included Rhythmic (isochronous) and Arrhythmic (non-isochronous) sequences (Fig. 1A). Each sequence was composed of 100 tones, 90% of which were standard tones (F0 = 500 Hz), and 10% were target tones. Two adjacent target tones were separated by 6–12 standard tones. Target tone F0s were presented at 7 different levels, specifically PSE + [-5Δ, -3Δ, -Δ, 0, +Δ, +3Δ, +5Δ] (logarithmic scale), and there were 8 target tones at the -5Δ level and 7 target tones at each of the other levels in each condition of each run. A run consisted of 5 Rhythmic and 5 Arrhythmic sequences, randomly intermixed. Each participant completed 5 runs for a total of 50 sequences, for a total of 250 target tones in each of the Rhythmic and Arrhythmic conditions. The tones in Rhythmic sequences were presented isochronously with 500 ms IOI. In contrast, the tones in Arrhythmic sequences were presented with IOI uniformly random between 250 and 750 ms. The length of each Arrhythmic sequence was controlled to be between 48 and 52 s, matching the 50 s length of
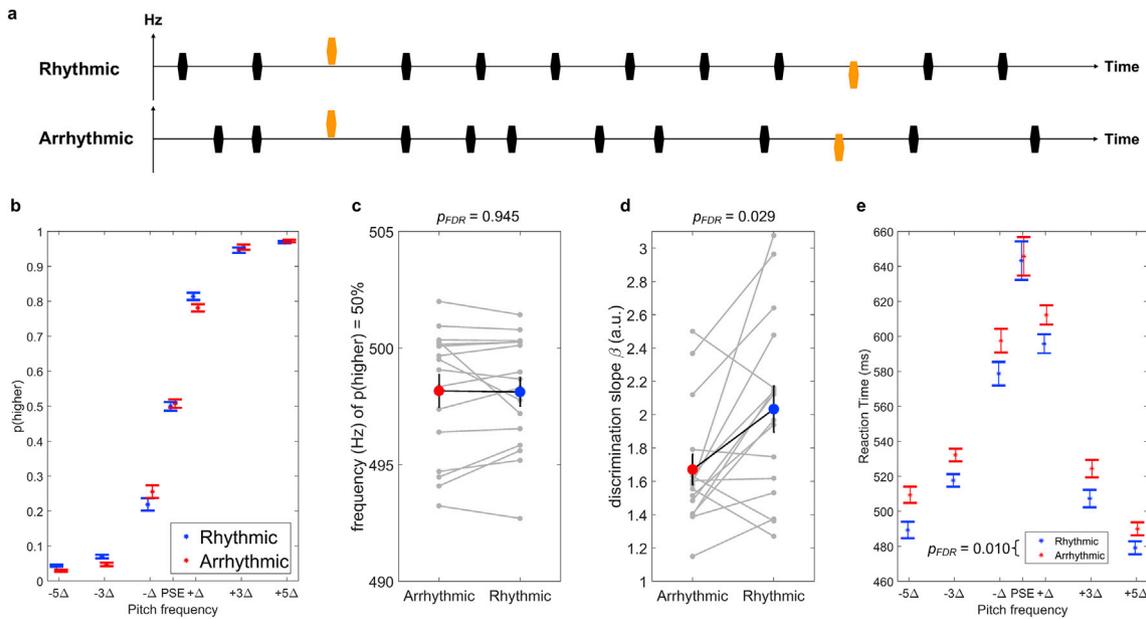
Fig. 1. Experimental design and behavioural performance. (A) Stimuli and task. In both conditions, 10% of tones were targets (yellow), which were higher or lower in pitch than standards (black) at a near-threshold. Participants judged whether target tones were higher or lower than standards. Tones in the Rhythmic sequence were isochronous with 500 ms IOI (inter-onset interval), and tones in the Arrhythmic (non-isochronous) sequence were presented with IOI uniformly random between 250 and 750 ms. Importantly, the IOI before and after each target tone was fixed at 500 ms in both conditions. (B) Psychometric performance on the perceptual judgment. For purposes of visualization, the error bars represent within-subject error (Cousineau, 2005) for the p(higher) at each level. Both PSE and Δ were individually determined by an initial adaptive psychophysical procedure. We fitted a logistic psychometric model for each participant's performance under each condition. Fitted parameters are presented in (C) and (D); each connected dot represents one participant's data, and the colored dots and error bars represent the mean ± standard error across participants. (C) The frequency of 50% responding "higher" (converted from α of logistic model) was not significantly different between Rhythmic and Arrhythmic conditions. (D) Discrimination sensitivity. The discrimination slope (β of logistic model) was significantly higher in the Rhythmic than Arrhythmic condition, suggesting participants have better pitch discrimination sensitivity in the Rhythmic than Arrhythmic context. (E) Response Time (RT). The correct trial RT on PSE ± [Δ, 3Δ, 5Δ] levels was shorter in the Rhythmic than Arrhythmic condition, suggesting rhythmic regularity facilitates behavioural response speed. Error bars represent within-subject error. For visual representation, RTs on PSE level were based on both correct and error trials, and RTs on other levels were based on only correct trials.

Rhythmic sequences. Importantly, the IOI before and after each target tone was fixed at 500 ms in both Rhythmic and Arrhythmic conditions to control for any possible effects of foreperiod or masking on behavioural or EEG responses (Rohenkohl et al., 2012; Cravo et al., 2013; Herrmann et al., 2016).

Target tones were presented 8.4 dB louder than standard tones, which served as a cue for the participant to respond. All participants were able to clearly detect this loudness change. Participants were instructed to judge whether the pitch of each loud (target) tone was higher or lower than the other (standard) tones, by pressing one of two buttons with their thumbs (right for higher and left for lower) on a controller, as accurately and as quickly as possible. Participants practiced this task in both conditions prior to the experimental session. The button pressed and reaction time (RT) of the first response within 1600 ms was recorded for each target tone. Ten participants who missed more than 3% of targets were considered to be not following the instructions (Fig. S1), and were not included in the n = 16 of the subsequent analyses. We used this strict exclusion criterion because most participants tended to miss responses when the target levels were difficult (around PSE). Therefore, a strict criterion made sure the participants included in the analyses had relatively low bias. After finishing a sequence, the next sequence started when the participant was ready and pressed a button. After every run, there was a mandatory break of at least 1 min before starting the next run. The experimental session lasted approximately 1 h.

2.4. Psychometric model fitting

Trials with premature response (RT < 200 ms) were excluded as missing responses. The proportion of "higher" response was calculated based on all trials that were responded to for each target level for each condition for each participant.

The psychometric data from each participant and condition was fitted by a function ψ, which combines a logistic model (*F*) and additional parameters for controlling lapse rate (Kingdom and Prins, 2010):

$$F(x; \alpha, \beta) = \frac{1}{1 + e^{-\beta(x-\alpha)}}$$

$$\psi(x; \alpha, \beta, \gamma, \lambda) = \gamma + (1 - \gamma - \lambda)F(x; \alpha, \beta)$$

which was defined by *x* (the frequencies of target tones on a logarithmic scale) and parameters α (the *x* point at which 50% of responses are "higher") and β (the slope of psychometric function, or discrimination sensitivity) of the logistical model, and additional parameters γ and λ (lapse rate, i.e., the probability of making an incorrect response independent of the stimulus intensity). In the first step, each of γ and λ was empirically fixed to the mean response at [-5Δ, -3Δ] or [+3Δ, +5Δ] levels for each model (lapse rate was measured at the extreme target levels but lapses can occur at any target level). Second, the fitting of free parameters α and β of function ψ was implemented with PAL_PFML_Fit function in Palamedes toolbox (RRID: SCR_006521) (Prins and Kingdom, 2009), which iteratively searches the best-fitted parameters across parameter space using a maximum likelihood criterion. Goodness of fit for each participant was estimated by comparing predicted and observed accuracy, with $R^2 > 95\%$. The individual perceptual judgment performances and the fitted psychometric functions are shown in Fig. S2.

2.5. Electroencephalographic recording and preprocessing

The EEG was sampled at 2048 Hz (filtered DC to 417 Hz) using a 128-

channel Biosemi Active Two amplifier (Biosemi B.V., Amsterdam). The electrode array was digitized (Polhemus Fastrak) for each participant prior to recording. EEG data were stored as continuous data, and transformed to an average reference offline. In subsequent steps, the EEG data was processed in MATLAB using the FieldTrip toolbox (RRID: SCR_004849) (Oostenveld et al., 2011).

We employed independent component analysis (ICA) to remove artifact signals (Jung et al., 2000). For performing ICA, we filtered the continuous EEG data 0.7–100 Hz and segmented it into −3 to 54 s time windows, time-locked to the first tone of each sequence. The ICA was performed on all sequences of each participant, and the components reflecting artifact, including eye blinking, eye movement, electrocardiogram, and 60-Hz powerline noise, were identified by visual inspection. Once obtaining the unmixing and mixing matrices from ICA, we went back to the unfiltered data, projected it to ICA space, removed the artifact components as identified above, and then the data was projected back to 128-channel space for all subsequent analyses. We used a subsequent 120 μV criterion on epochs to exclude the ones containing artifacts which were not removed by ICA, with removal rate ranging between 0.2 and 17.0% across participants. To facilitate the speed of subsequent processes, the data was downsampled to 256 Hz.

2.6. Modeling dipole sources for auditory cortex

We employed a dipole source model as a spatial filter in order to extract the EEG signal generated from left and right auditory cortices, following previous studies (Fujioka et al., 2012; Chang et al., 2016, 2018). In the present study, we were primarily interested in responses from auditory cortex, so we analyzed the EEG signals in source space rather than from surface channels, by extracting the oscillatory signals generated from left and right auditory cortices while attenuating signals generated from other brain regions.

Using dipole source modelling enabled us to perform hypothesis driven analyses on the EEG signal generated primarily from bilateral auditory cortices. Most previous entrainment studies that analyze surface electrodes either select the electrodes that have maximum auditory ERP responses or are known to reflect auditory responses, such as frontocentral electrodes, and these studies interpret the results as generated from auditory cortex (e.g., Henry et al., 2014; ten Oever et al., 2017). The dipole approach has advantages in that it is a linear weighting of all the surface electrodes that emphasizes the response from auditory cortex. It also enables assessment of hemispheric effects. Using auditory cortical sources is appropriate as electrophysiological evidence from monkeys shows that delta entrainment is observed in auditory cortex (Lakatos et al., 2013; Calderone et al., 2014), giving a physiological basis for focusing on the auditory EEG source.

We estimated the locations of bilateral auditory cortices by localizing the P1 ERP (event-related potential) component. First, the continuous EEG data was band-pass filtered 0.7–40 Hz and then segmented into −100 to 200 ms epochs, time locked to standard tone onset in all sequences, which were averaged into ERP (event-related potential) waveforms and used to model dipole sources. Second, two auditory cortex sources were estimated for each participant for the auditory evoked P1 (~60–90 ms) with the dipole locations constrained to be symmetric across hemispheres in location but not orientation, using the multiple source probe scan algorithm and the four-shell ellipsoid model included in the Brain Electrical Source Analysis (BESA, RRID: SCR_009530) software package. P1 was chosen because it is the dominant peak at fast presentation rates (N1 peaks are strongly reduced at fast rates; Näätänen and Picton, 1987), and is generated primarily from primary auditory cortex (Godey et al., 2001). The mean locations of fitted dipoles across participants were at Talairach coordinates [±45.6, −14.9, 23.8] with approximate mean orientations [0.0, 0.7, 0.7] and [0.1, 0.8, 0.6] for left and right dipoles. These locations are close to bilateral primary auditory cortices (far below the 1 cm averaged error range of four-shell head model; Slotnick, 2004) with orientations toward the mid-frontal surface

area, consistent with typical auditory evoked potentials. The mean residual variances of the source fittings was 9.7% (range 2.4–19.6%). Finally, using the dipole model, the unfiltered continuous 128-channel EEG was projected into source-space EEG for further time-frequency analyses. Note that the current procedure only ensures that the source-space EEG signals are dominantly generated in the auditory cortex, given the low residual variances of the source fitting. Considering the spatial specificity of EEG, brain signals generated from the neighboring areas may contribute to the source waveforms, but they should have a relatively small contribution compared to the auditory brain signals.

2.7. Delta band (1–3 Hz) analyses

We were interested in the delta phase during the pre-target interval, which has been shown to phase-lock with the stimulus presentation rate and thus reflect temporal entrainment. To initially identify whether low-frequency oscillations in the EEG entrained to the presentation rate of the auditory sequence, we frequency transformed each unfiltered 50 s sequence, using 0.1 Hz frequency bins ranging 1–7 Hz and a Hanning taper to avoid edge artifacts.

To isolate the delta band, we filtered the continuous source-space EEG at 1–3 Hz with Butterworth (zero-phase, third order) high-pass and low-pass filters, performed a Hilbert transform to obtain the instantaneous phase, and then segmented into −1.5 to 1.5 s epochs, time-locked to target onsets. We used the Butterworth filter because we aimed to create a narrow band-pass filter while minimizing ripple effects in the time domain signal (Widmann et al., 2015), which follows previous studies with similar purposes (Besle et al., 2011; Ng et al., 2012a, 2012b; Cravo et al., 2013; Tal et al., 2017).

The inter-trial phase clustering (ITPC), sometimes referred to as the phase-locking value or phase coherence, was used to measure the phase distribution of delta band at each time point across trials (Cohen, 2014), which ranges from 0 (circular-uniformly distributed phases) to 1 (perfectly identical phases). Higher ITPC of delta phase represents more precise phase entrainment (Tal et al., 2017; ten Oever et al., 2017).

To correlate delta phase and pitch discrimination sensitivity, we first ordered the trials based on the sum of absolute phase deviations from the mean phase (the aligned phase of delta entrainment) at each time point across the pre-target interval (−0.5 to 0 s), and then binned the ordered trials into 10 bins (with 50% of trials overlapped across adjacent bins), within each target level, condition, and participant. Second, we estimated the pitch discrimination sensitivity (β or slope) by modeling the behavioural performance with psychometric function (as described in *Psychometric model fitting*) for each bin across all target levels. Third, we performed a Spearman rank correlation between ranked absolute phase deviation and pitch discrimination sensitivity, and obtained a Spearman rank correlation coefficient for each participant and condition. Finally, each correlation coefficient was further z-normalized to a bootstrapped null distribution for each condition and participant. Each null distribution was built by performing the same preceding steps on randomly paired behavioural response and delta phase deviation across trials for 1000 iterations within each target level, which represented the null distribution of an uncorrelated effect. In sum, more negative z-values (z-normalized Spearman rank correlational coefficient) indicate a higher association between better pitch discrimination sensitivity and pre-target delta phase being closer to the entraining phase (optimal phase).

To correlate delta phase and RT, we performed a linear correlation between RT and the absolute phase deviation in the pre-target interval across all correct trials, within each target level, condition, and participant. Each observed correlation coefficient was further z-normalized to a bootstrapped null distribution. Each null distribution was built as above by randomly pairing RT and delta phase deviation across trials for 1000 iterations, which represented the null distribution of an uncorrelated effect. A mean z-value for each condition and participant was obtained by averaging z-normalized correlational coefficients across target levels. We only include the PSE ±Δ and ±3Δ target levels, because the levels at PSE

±5Δ were very easy to discriminate, and the pitch of target tones at the PSE level was not perceptually discriminable from the pitch of standard tones. The mean standard deviation of RT across participants at ±5Δ levels was 113.81 ± 9.99 ms, which is smaller than the mean standard deviation of RT at ±3Δ and ±Δ levels, which was 146.86 ± 11.44 ms (t(15) = −5.23, p < 0.001). The smaller RT variance at the ±5Δ levels likely reflects near ceiling performance. In sum, higher mean z-values indicate that pre-target delta phases that are closer to the entraining phase (optimal phase) are associated with faster (shorter) RTs to the target.

2.8. Beta band (15–25 Hz) analyses

We were interested in the induced (non-phase-locked) power in beta band in the pre-target interval. Previous studies show that power decreases (desynchronization) and increases (resynchronization) to entrain to the rate of the beat of an externally presented tone sequence, and thus reflects temporal prediction (Snyder and Large, 2005; Iversen et al., 2009; Fujioka et al., 2009, 2012; Cirelli et al., 2014; Fujioka et al., 2015, but see Meijer et al., 2016). To obtain induced activities, the trial-averaged ERP waveform of −1.5 to 1.5 s around target tone onset was subtracted from each target epoch within each condition and participant (Fujioka et al., 2012; Cohen, 2014; Chang et al., 2016, 2018). The Morlet wavelet transformation was performed on each target epoch of induced activities (frequency bin size = 1 Hz; 10 cycles). The beta power was baseline corrected by percentage change to the mean power in the pre-target interval for each frequency bin, and the beta power time series was obtained by averaging induced power across 15–25 Hz. Edge artifacts did not affect the time-frequency activities at the pre-target interval.

Following our previous studies (Fujioka et al., 2012; Chang et al., 2018), for each condition, we first identified the latency of beta desynchronization (decrease in power) as the time point with minimum beta power within the pre-target interval and the resynchronization (power rebound following the desynchronization) as the time point with beta power closest to the baseline (0% power change) between the latency of desynchronization and time point 0 s.

To describe the shape of beta power modulation for each trial, we fitted a quadratic (parabola) function ($y = ax^2 + bx + c$) on the induced beta power time series in the pre-target interval (data was centered and scaled, and fitted with bisquare weights method). The fitted quadratic coefficient (a) reflects the modulation peak-trough shape of beta power, with more positive values representing U-shaped modulation with deeper troughs, 0 representing linear shape, and more negative values representing ∩-shaped modulations with higher peaks. The vertex position ($-b/2a$) estimates the beta desynchronization latency. The mean R^2 of fitting across participants was 59.6 ± 0.6%. This approach allows us to simply use one parameter to quantify the peak-trough shape, and one parameter to quantify the vertex latency of the beta power fluctuation, which is suitable to model single-trial neural activities and perform trial-by-trial EEG-behaviour correlations. This approach is better than a peak-searching approach at a single-trial level as it acts like a low-pass filter; it avoids identifying spurious noise peaks while extracting the slow modulation shape and vertex.

To correlate the size of the beta modulation trough or desynchronization latency with pitch discrimination sensitivity, following the procedure described above, we ordered and binned the trials into 10 bins (with 50% of trials overlapped across adjacent bins), based on each fitted beta modulation index (quadratic coefficient or vertex position), within each target level, condition, and participant, and then estimated the pitch discrimination sensitivity (β, slope) for each bin across target levels. We performed a Spearman rank correlation between each ranked beta modulation index and pitch discrimination sensitivity across target levels, and further z-normalized to a bootstrapped null distribution for each participant and condition. In sum, for the beta power modulation shape, higher z-values show a greater association between deeper pre-

target beta modulation trough (ideal U-shaped beta power) and better pitch discrimination sensitivity. For the beta desynchronization latency, higher z-values show a greater association between later beta desynchronization latency and better pitch discrimination sensitivity.

To correlate beta modulation shape with RT, following the procedure described above, each beta modulation index was linearly correlated with RT across trials within each target level, normalized to z-value (the bootstrapped null distribution of randomly paired RT and quadratic coefficients across trials). A mean z-value was obtained for each condition and participant by averaging z-values across target levels. In sum, for the beta power modulation shape, lower mean z-values indicate a greater association between deeper pre-target beta modulation trough (ideal U-shaped beta power) and faster (shorter) RT. For the beta desynchronization latency, lower mean z-values indicate a greater association between later beta desynchronization latency and faster (shorter) RT.

2.9. Delta-beta coupling analyses

Given that both delta phase and beta power modulation are affected by rhythmic regularity, we were interested in the cross-frequency phase-amplitude coupling (PAC) between delta and induced beta activities. Phase-amplitude coupling is thought to result from the excitatory or inhibitory phase of neural circuits oscillating at low-frequencies affecting the power of high-frequency oscillations (Hyafil et al., 2015). To estimate the delta-beta coupling, we employed the dPAC index, which was calculated for each trial across time points,

$$dPAC = \left| \frac{1}{n} \sum_{t=1}^{n} A_t \left(e^{i\varphi_t} - \frac{1}{n} \sum_{t=1}^{n} e^{i\varphi_t} \right) \right|$$

where the n signifies the total number of time points, A_t the power amplitude of modulated frequency, and φ_t the phase of the modulating frequency at time point t. The dPAC is the debiased version of the widespread PAC method (Canolty et al., 2006) for solving phase clustering bias (van Driel et al., 2015). In the present study, we estimated dPAC with reversed beta power polarity to reflect the modulation trough rather than peak. Each observed dPAC was further transformed into a z-value (dPACz) by comparing with 1000 time-shuffled dPAC (null distribution).

To correlate delta-beta coupling with pitch discrimination sensitivity, following the procedure described above, the dPACz values were rank-correlated with discrimination sensitivity across 10 dPACz-ranked bins (with 50% of trials overlapped across adjacent bins), and then a z-normalized correlational coefficient (relative to the bootstrapped null distribution) was obtained for each condition and participant. In sum, a higher z-value indicates a greater association between better delta-beta coupling and better pitch discrimination sensitivity.

To correlate delta-beta coupling with RT, the dPACz scores were linearly correlated with RT across trials within each target level, normalized to z-values (relative to the bootstrapped null distribution). A z-value was obtained for each condition and participant by averaging z-values across target levels. In sum, lower mean z-values indicate a greater association between better delta-beta coupling and faster (shorter) RT.

2.10. Partial out covariances among EEG indexes for EEG-behaviour correlations

The covariances were relatively small among the EEG indexes (delta phase deviation, quadratic coefficient of beta power modulation peak-trough shape, vertex latency of beta desynchronization, and dPACz) across the two hemispheres (see Supplementary Material and Table S1). However, to exclude any potential confounding effects among these co-variances on the EEG-behaviour correlations, each EEG index of each hemisphere was partialled out by all remaining indexes across both hemispheres (taking the residuals from a regression model in which each

EEG index was predicted by all other indexes), prior to each abovementioned correlational analysis. The only exception was that the quadratic coefficient and the vertex latency of the beta power modulation shape were not partial out from each other, because these two indexes are mathematically dependent in the quadratic function.

2.11. Experimental design and statistics

Participant (n = 16) was the random factor for the within-subject statistical tests in the current study. The assumptions of parametric tests were checked (Kolmogorov-Smirnov test with threshold $p < 0.01$), and the alternative test or non-parametric permutation tests (1000 iterations) were used when the assumptions were violated. The test being used is specified below for each p-value. The statistical tests were performed by MATLAB (2015b) or R (3.3.3). Statistical decisions were based on two-tailed tests. Multiple comparisons of all the planned statistical tests of the current study were controlled by experiment-wise false discovery rate (FDR) (Benjamini and Hochberg, 1995; Luck and Gaspelin, 2017), and each corrected p-value was reported as p_{FDR}.

To access the EEG-behaviour trial-by-trial correlational effects, we performed statistical tests on the z-normalized correlational coefficients across participants. It is important to note that we did not test the statistical significance of each within-participant correlational coefficient, but we tested whether the within-participant correlational effect was consistent across all participants. In other words, for each condition, we used a one-sample t-test to assess whether the z-normalized correlational coefficients across participants were significantly different from 0 in the same direction. This approach is statistically similar to a linear mixed-effect model with random intercepts and slopes, which assesses the influence of predictors of interest while taking into account the variance across participants (Barr et al., 2013). The current approach fits our purpose better than a linear mixed-effect model because it can incorporate non-parametric rank correlation and bootstrapping z-normalization. Note that the trial-by-trial correlational analyses were only performed within the Rhythmic condition, as we aimed to investigate how neural activities anticipatorily associate with perceptual performance, when rhythmic temporal regularity is available. An extended question is whether rhythmicity moderates these EEG-behaviour relationships, that is, whether such a relationship would be diminished in the Arrhythmic compared to Rhythmic conditions. We therefore performed post-hoc analyses to investigate this question, and the results are reported in the *Supplementary Material*.

3. Results

3.1. Behavioural performance and psychometric modeling

The psychometric modeling results showed that rhythmic regularity facilitated pitch discrimination sensitivity (Fig. 1B). The frequency of 50% responding "higher" (converted from α of logistic model) was not significantly different between Rhythmic and Arrhythmic conditions (t(15) = −0.16, $p_{FDR} = 0.945$, paired t-test; Fig. 1C). The discrimination slope (β of logistic model) was significantly higher in the Rhythmic than Arrhythmic condition (t(15) = 2.97, $p_{FDR} = 0.029$, paired t-test; Fig. 1D), suggesting that participants have better pitch discrimination sensitivity in the rhythmic than arrhythmic context. This is equivalent to saying the required frequency difference to achieve 70.7% pitch discrimination accuracy decreased 11.5% ± 5.3% on a logarithmic frequency scale, comparing the Rhythmic to Arrhythmic conditions. This effect size is at the same level (approximately 10%) as other similar behavioural studies (Haegens and Zion Golumbic, 2018).

The RT results are shown in Fig. 1E. A repeated measure MANOVA (alternative ANOVA without sphericity assumption, O'Brien and Kaiser, 1985) on RT (correct trials only) with variables Rhythmicity (Rhythmic, Arrhythmic) and Target Levels (PSE ± [Δ, 3Δ, 5Δ]) showed significant main effects of Rhythmicity (Wilks(1) = 0.49, approximate F(1,

15) = 15.55, $p_{FDR} = 0.010$) and Target Level (Wilks(1) = 0.12, approximate F(5,11) = 15.83, $p_{FDR} = 0.002$), but no interaction effect (Wilks(1) = 0.95, approximate F(5,11) = 0.11, $p_{FDR} = 0.988$). A linear trend analysis (collapsing Rhythmicity) further showed that RTs are longer when the target level is closer to the PSE (t(15) = 9.39, $p_{FDR} < 0.001$) as expected. As for the main effect of Rhythmicity, the averaged RT across target levels (excluding the PSE level) in the Rhythmic condition was 16.3 ms shorter than in the Arrhythmic condition, indicating that temporal regularity facilitates behavioural response speed. This effect size is similar to previous studies reporting that rhythmicity facilitates RT (e.g., Morillon et al., 2016).

3.2. Beta power modulation is affected by rhythmicity and associates with pitch discrimination sensitivity

We were interested in the induced (non-phase-locked) power activities in beta band (15–25 Hz) in the pre-target interval, as previous studies showed that beta power decreases (desynchronization) and increases (resynchronization) so as to entrain to the rate of the beat of an externally presented tone sequence, and thus reflects temporal prediction (Snyder and Large, 2005; Iversen et al., 2009; Fujioka et al. 2009, 2015, 2012; Cirelli et al., 2014). Replicating these previous studies, the induced beta power fluctuations in bilateral auditory cortices (Fig. 2A) showed that power decreased following the onset of a standard tone, and then increased in anticipation of the upcoming target tone, prior to the 0 ms point. In the left auditory cortex, the desynchronization latency was earlier in the Arrhythmic than Rhythmic condition (t(15) = −2.88, $p_{FDR} = 0.032$, permutation test), as was the resynchronization latency (t(15) = −2.70, $p_{FDR} = 0.046$, permutation test) (Fig. 2B). There were no significant latency effects in the right auditory cortex (t-values < 1.26 and p-values$_{FDR}$ > 0.347, permutation test; Fig. 2B). The resynchronization latency difference is consistent with a previous study (Fujioka et al., 2012) that found that resynchronization latency is earlier in arrhythmic than rhythmic conditions. It was suggested that the beta power resynchronization latency adapts to the onset time of the next tone when it is temporally predictable, but when timing is uncertain, beta resynchronization reflects preparation for the possibility of an early tone onset (Fujioka et al., 2012). The current study was not a full replication of the previous study, as we did not include variation in the stimulus presentation rate. Nevertheless, the current findings are consistent with the previous study, suggesting that beta power modulation in the Rhythmic condition reflects temporal prediction and thus is consistent with beta power reflecting entrainment.

Beyond replicating the effects of latencies, additional exploratory analyses did not showed any differences on beta desynchronization depth between Rhythmic and Arrhythmic conditions in either left (−6.61 ± 0.74 vs. −5.16 ± 0.48, t(15) = −1.38, $p_{FDR} = 0.338$, permutation test) or right (−6.65 ± 0.65 vs. −6.41 ± 0.61, t(15) = −0.32, $p_{FDR} = 0.869$, permutation test) auditory cortex.

We further investigated whether pre-target beta power modulation indexes are anticipatorily associated with perceptual performance, as our previous study showed that the depth of the beta power modulation trough reflects expectations for pitch (Chang et al., 2018). In the present paper, at a trial-by-trial level, we correlated both pitch discrimination sensitivity and RT with the depth of the beta trough (the depth of the U-shaped fluctuation) or beta desynchronization latency in the Rhythmic condition, where the rhythmic temporal regularity is available. The power modulation was modeled by a quadratic (parabola) function, and the U-shaped fluctuation depth and vertex (desynchronization) latency are represented by fitted coefficients (see *Method: Beta band (15–25 Hz) analyses* for details).

The correlational analyses on beta modulation depth and discrimination sensitivity (Fig. 3A) showed that, in left auditory cortex, deeper beta modulation troughs are associated with increased pitch discrimination sensitivity (t(15) = 3.10, $p_{FDR} = 0.025$, one-sample t-test). The same analyses in right auditory cortex did not show a significant result
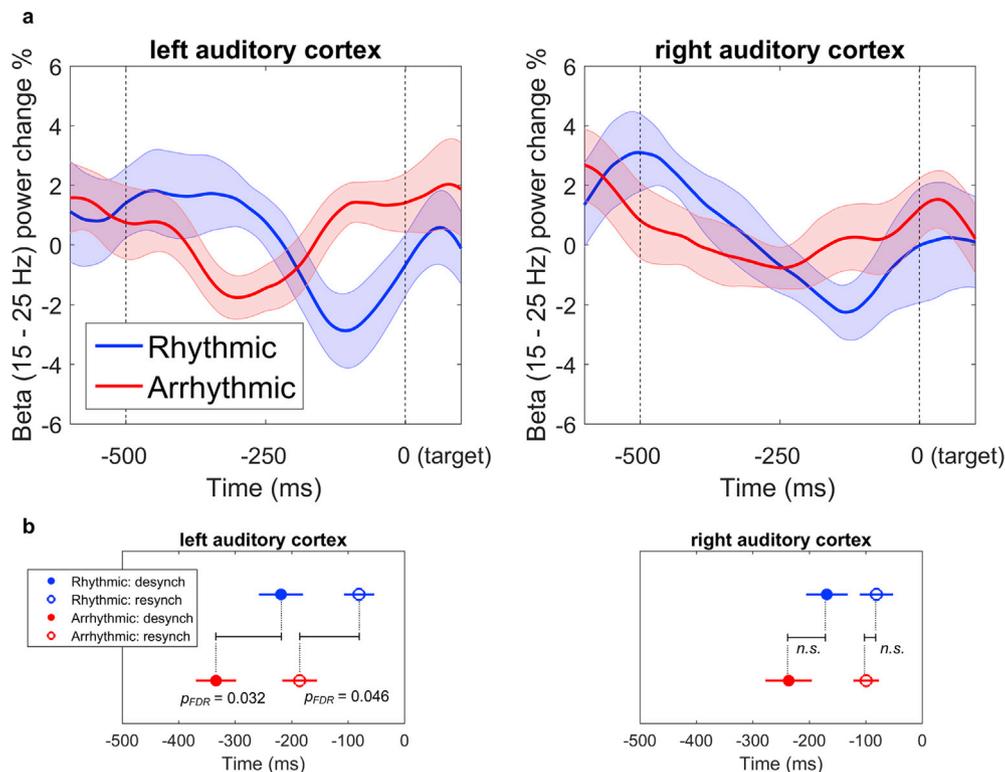
Fig. 2. Beta power modulation is affected by rhythmicity. (A) Beta power (15–25 Hz) decreases (desynchronization) following the onset of a standard tone, and then increases (resynchronization) again in anticipation of the upcoming target tone. (B) Beta desynchronization and resynchronization latencies were both earlier in the Arrhythmic than Rhythmic condition in left auditory cortex (but not in the right auditory cortex). Error bars represent standard error of mean. (n.s.: non-significant).

($t(15) = -0.55$, $p_{FDR} = 0.741$, one-sample *t*-test). This effect was significantly stronger in left than right auditory cortex ($t(15) = 2.62$, $p_{FDR} = 0.045$, paired *t*-test). On the other hand, depth of the beta modulation trough was not significantly related to RT (Fig. 3B) for either left ($t(15) = 1.05$, $p_{FDR} = 0.474$, one-sample *t*-test) or right ($t(15) = 0.10$, $p_{FDR} = 0.969$, one-sample *t*-test) auditory cortex.

The correlational analyses on beta desynchronization latency and discrimination sensitivity did not show any significant results (left: $t(15) = 0.51$, $p_{FDR} = 0.750$; right: $t(15) = -0.96$, $p_{FDR} = 0.480$; one-sample t-tests; Fig. 3C). The correlational analyses on beta desynchronization latency and RT did not show any significant results either (left: $t(15) = -0.23$, $p_{FDR} = 0.909$; right: $t(15) = -0.94$, $p_{FDR} = 0.480$; one-sample t-tests; Fig. 3D).

In sum, induced beta power modulation is affected by the rhythmic regularity of the auditory sequence, and trial-by-trial analyses show that a deeper beta power modulation trough prior to a deviant pitch is anticipatorily associated with better pitch discrimination sensitivity.

3.3. Delta phase is modulated by rhythmicity but not associated with perceptual performance

We were interested in the delta (1–3 Hz) phase in the pre-target interval, which has been shown to phase-lock with stimulus presentation rate and thus reflect temporal entrainment (e.g., Tal et al., 2017; ten Oever et al., 2017). We first examined the frequency content of the unfiltered time-domain waveform in response to each stimulus sequence to confirm that delta oscillations entrained to the auditory presentation rate (2 Hz). The power spectrum (Fig. 4A) shows a clear peak at 2 Hz in the Rhythmic but not in the Arrhythmic condition (left auditory cortex: $t(15) = 2.80$, $p_{FDR} = 0.035$; right auditory cortex: $t(15) = 3.63$, $p_{FDR} = 0.020$; paired t-tests), as well as at harmonic frequencies of 4 and 6 Hz (t-values > 3.07, p-values$_{FDR} < 0.025$, paired t-tests). Thus this initial analysis shows delta oscillations entrain to the 2 Hz stimulus

presentation rate.

The ITPC (inter-trial phase clustering) was calculated on band-pass filtered waveforms (delta band 1–3 Hz) for both Rhythmic and Arrhythmic conditions (Fig. 4B). The group-mean ITPC for each condition in our study was around the same level reported in previous studies (e.g., Henry and Obleser, 2012; ten Oever et al., 2017), suggesting that we observed a robust delta-band ITPC signal at auditory dipoles of similar magnitude as in previous studies. The mean ITPC across the pre-target interval was higher in Rhythmic than Arrhythmic conditions in both left ($t(15) = 1.98$, $p_{FDR} = 0.046$, permutation test) and right ($t(15) = 3.67$, $p_{FDR} = 0.023$, permutation test) auditory cortices. This finding replicates previous studies showing that the delta phase phase-locks to the rhythmic regularity in the auditory input. The reason we averaged the ITPC across the entire pre-target interval rather than reporting the ITPC time series results was because the beta power modulation and dPACz indexes considered the entire pre-target interval, and we wanted the ITPC index to represent the information over the same time-interval.

An interesting observation is that some previous studies reported a stronger rhythmicity effect on ITPC using surface electrodes than our findings using auditory dipoles (e.g., ten Oever et al., 2017). However, as we aimed to investigate delta entrainment activities generated by auditory cortex, analyzing ITPC using surface electrodes is a suboptimal approach for the current study, because surface electrodes will likely include delta entrainment signals generated from other brain regions (Besle et al., 2011; Morillon and Baillet, 2017).

We further investigated whether the pre-target delta phase was anticipatorily associated with subsequent perceptual performance. On a trial-by-trial level, we separately correlated pitch discrimination sensitivity and RT with the phase deviation on each trial, relative to the mean phase in the Rhythmic condition (see *Method: Delta band (1–3 Hz) analyses* for details). If the mean (entrained) phase prior to a target represents the optimal neural status for anticipatorily facilitating perceptual
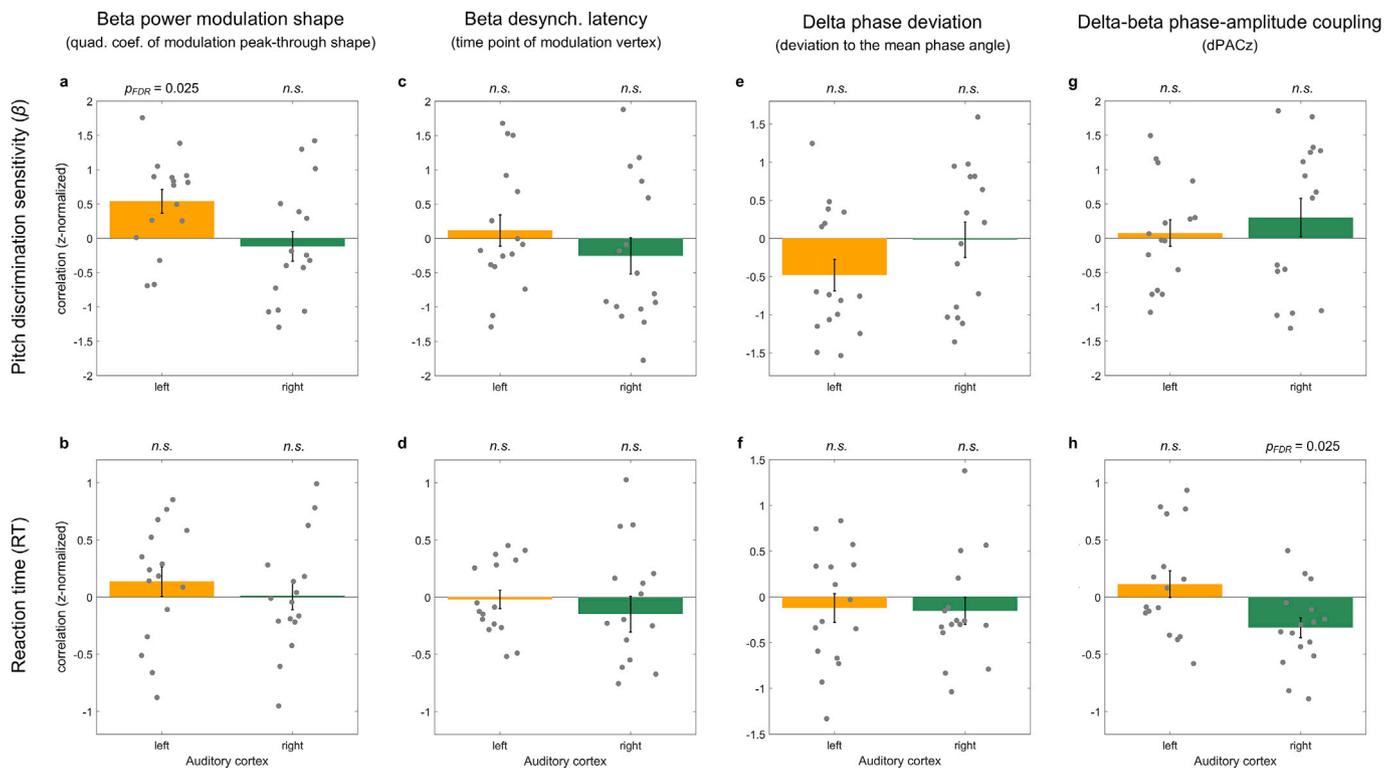
Fig. 3. Distributions of trial-by-trial correlational strength between pre-target neural oscillatory activities and behavioural performance on the target tone in the Rhythmic condition. For the beta power on each trial, we modeled the pre-target beta power modulation peak-trough shape with the quadratic coefficient (quad. coef.) of a quadratic (parabola) function. The beta desynchronization (desynch.) latency was also estimated by the vertex of the same quadratic function. For the delta phase on each trial, we extracted the absolute phase deviation from the mean phase (the aligned phase of delta entrainment) across the pre-target interval. The dPACz index was used to estimate the delta-beta phase-amplitude coupling strength on each trial. For each participant, trial-by-trial neural activities were correlated with discrimination sensitivity and with RT, after the covariances among these EEG indexes were partialed out (see Methods for details). (A–H) The distribution of correlational strengths across participants is presented as dots, and the mean ± standard error across participants is presented as bar graphs ± error bars. Results showed that (A) deeper pre-target beta power U-shaped modulation trough in left auditory cortex predicts better pitch discrimination sensitivity, and (H) better pre-target delta-beta coupling in right auditory cortex predicts faster RT. (n.s.: non-significant).

performance, then pre-target intervals with delta phase closer to the mean phase should associate with better subsequent perceptual performance (e.g., Henry and Obleser, 2012). However, our results did not show such an effect. Phase deviation was not significantly correlated with discrimination sensitivity, although there was a trend in the left auditory cortex (Fig. 3E; left auditory cortex: t(15) = −2.32, p_{FDR} = 0.067; right auditory cortex: t(15) = −0.07, p_{FDR} = 0.970, one-sample t-tests). Phase deviation was not significantly correlated with RT either (Fig. 3F; left auditory cortex: t(15) = −0.77, p_{FDR} = 0.583; right auditory cortex: t(15) = −1.03, p_{FDR} = 0.474, one-sample t-tests).

Together, the analyses replicated previous studies in that the 2 Hz delta oscillations entrained to the rhythmic regularity of the tone sequence, and the ITPC of the delta phase was higher in the Rhythmic than Arrhythmic condition. However, unlike previous studies showing that delta phase is associated with perceptual performance for auditory intensity and timing (Henry and Obleser, 2012; Henry et al., 2014; Arnal et al., 2015; ten Oever et al., 2017; Bauer et al., 2018), the present results suggest that delta phase entrainment is not strongly related to near-threshold pitch perception performance.

3.4. Delta-beta phase-amplitude coupling is modulated by rhythmicity and associates with RT

Given that both delta phase and beta power modulation are affected by rhythmic regularity, we were interested in, first, whether the degree of delta-beta phase-amplitude coupling (indexed by dPACz, where higher dPACz values reflect better delta-beta coupling; see *Method: Delta-beta coupling analyses* for details) related to the rhythmicity of the input

sequence. Results showed that the dPACz was higher in the Rhythmic than Arrhythmic condition in both left (t(15) = 4.85, p_{FDR} = 0.003, paired t-test) and right (t(15) = 3.69, p_{FDR} = 0.016, paired t-test) auditory cortices (Fig. 5).

We further investigate whether delta-beta coupling in the pre-target period is anticipatorily associated with subsequent perceptual performance, by correlating dPACz separately with pitch discrimination sensitivity and RT on a trial-by-trial level in the Rhythmic condition (Fig. 3H). The results showed that dPACz and RT are negatively correlated in the right auditory cortex (t(15) = −3.06, p_{FDR} = 0.025, one-sample t-test), indicating that the higher the coupling strength, the shorter the RTs. The same analyses did not show any significant effects in left auditory cortex (t(15) = 0.97, p_{FDR} = 0.480, one-sample t-test). This effect was stronger in right than left auditory cortex (t(15) = 2.55, p_{FDR} = 0.046, paired t-test). For pitch discrimination sensitivity, there were no significant correlations in either left (t(15) = 0.39, p_{FDR} = 0.826, one-sample t-test) or right (t(15) = 1.08, p_{FDR} = 0.474, one-sample t-test) auditory cortices (Fig. 3G).

Together, the analyses of delta-beta phase-amplitude coupling showed, first, that coupling strength was higher for Rhythmic than Arrhythmic sequences and, second, that higher coupling strength is anticipatorily associated with shorter RT in a subsequent pitch discrimination judgment on a trial-by-trial level.

4. Discussion

Accurate pitch perception is crucial for identifying objects in the world and perceiving speech and music. We showed that rhythmic
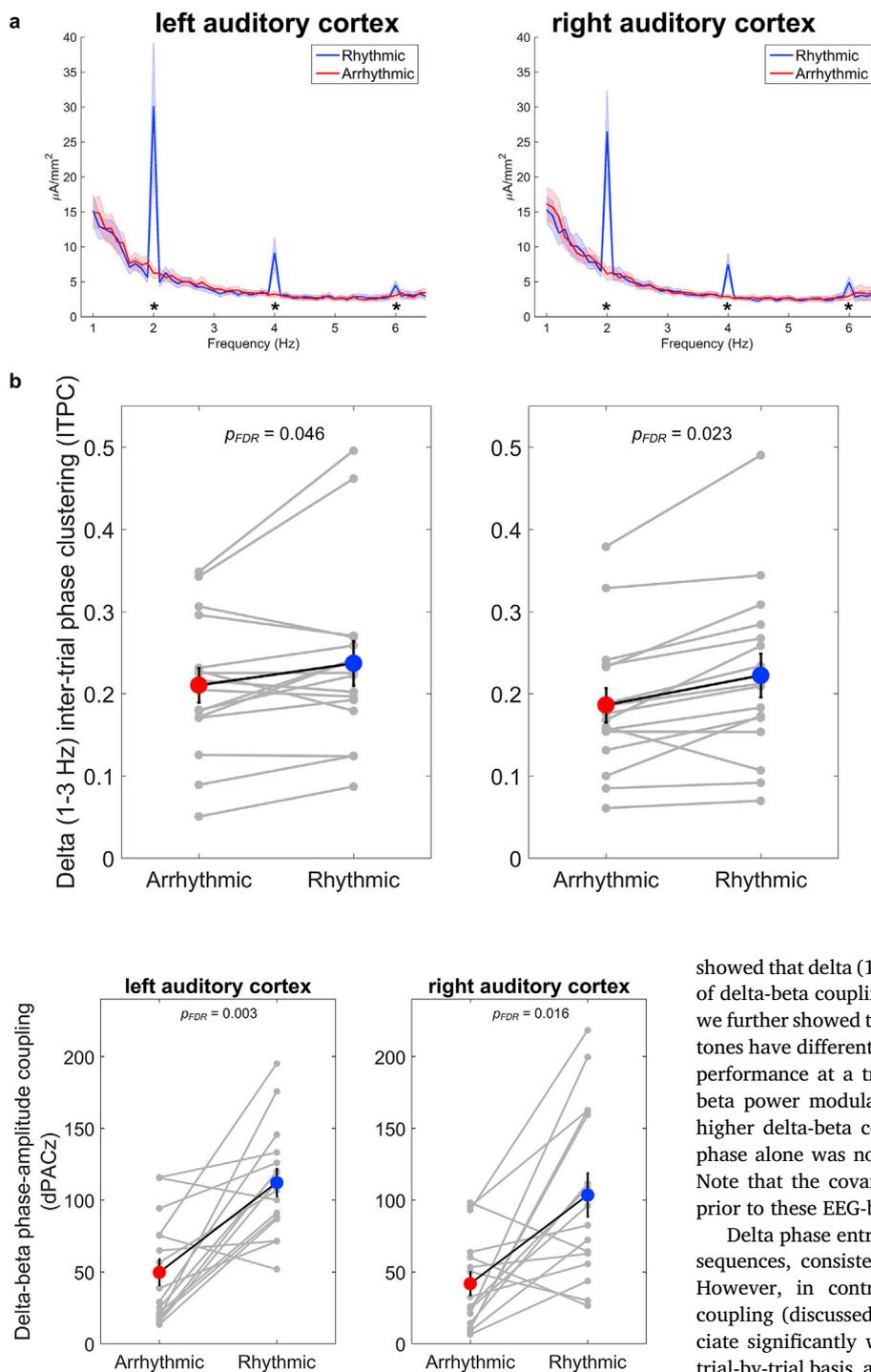
Fig. 4. Delta phase entrains to rhythmic regularity. (A) A frequency transformation of the unfiltered auditory EEG signal (extracted from auditory cortex) for each individual sequence (~50 s) for each condition showed that the power at 2 Hz was stronger in the Rhythmic than Arrhythmic condition in both cortices. (*: $p_{FDR} < 0.05$) (B) We further band-passed filtered the signal at the delta range (1–3 Hz) and then obtained the instantaneous phase with a Hilbert transform. The inter-trial phase clustering (ITPC) averaged over the pre-target interval was obtained for each condition and participant. ITPC ranges between 0 and 1, where 1 represents perfect phase-locking across trials, and 0 represents uniformly distributed phase across trials. The results showed that ITPC was higher in Rhythmic than Arrhythmic condition in both cortices. Each connected dot represents one participant's data, and the colored dots and error bars mean ± standard error across participants.

Fig. 5. Pre-target delta-beta phase-amplitude coupling is modulated by rhythmicity. Higher dPACz values represent higher phase-amplitude coupling strength between the phase of low-frequency oscillations (delta: 1–3 Hz) and the power of high-frequency oscillations (beta: 15–25 Hz). The dPACz value of each participant is shown as connected dots, and the mean ± standard error across participants by colored dots. The result showed dPACz is higher in the Rhythmic than Arrhythmic condition in both cortices.

regularity facilitates fine pitch discrimination, and revealed how it is implemented in neural entrainment activities. Participants discriminated near-threshold pitch deviations (targets) in contexts where tones were either rhythmically or arrhythmically sequenced. The behavioural results showed rhythmic regularity facilitates both psychophysical pitch discrimination sensitivity and reaction time (RT). The EEG analyses showed that delta (1–3 Hz) phase, beta (15–25 Hz) power, and the degree of delta-beta coupling were all modulated by rhythmicity. Interestingly, we further showed that these neural activities immediately prior to target tones have differential behavioural contributions to pitch discrimination performance at a trial-by-trial level. Specifically, (1) deeper U-shaped beta power modulation predicts higher discrimination sensitivity, (2) higher delta-beta coupling strength predicts shorter RT, but (3) delta phase alone was not related to either discrimination sensitivity or RT. Note that the covariances among the EEG indexes were partialed out prior to these EEG-behaviour correlational analyses.

Delta phase entrained (phase-locked) to the rhythmicity in the input sequences, consistent with previous studies (Calderone et al., 2014). However, in contrast with beta modulation depth and delta-beta coupling (discussed below), degree of delta entrainment did not associate significantly with perceptual discrimination of pitch or RT on a trial-by-trial basis, although there was a trend for an association between higher pitch discrimination sensitivity and smaller delta phase deviation in the left hemisphere. In contrast, previous studies have found robust associations between delta phase and the perception of timing or intensity deviations (Henry and Obleser, 2012; Henry et al., 2014; Arnal et al., 2015; ten Oever et al., 2017; Bauer et al., 2018). Thus, there might be a distinction in how delta phase entrainment relates to spectral-based (involving frequency and pitch) and temporal/intensity-based (involving onsets, intensity changes, duration and rhythm) perceptual sensitivity, although additional studies need to be done that directly compare associations between delta phase and pitch, timing and intensity. If found, such a distinction would be interesting as, at a more abstract level, pitch is more related to the content or identity of a sounding auditory object, whereas timing and intensity are more related to an object's location in time and space, suggesting that delta phase may relate more to timing

than to perceptual facilitation of a sounding object's identity. Note, of course, that these post-hoc speculations are based on null statistical differences and should therefore be taken with caution. It is possible that a correlation between delta phase and perceptual facilitation might be observed with a larger sample size. However, given the same statistical power, beta modulation shape and delta-beta coupling were more strongly associated with pitch discrimination performance than delta phase.

With respect to beta, we found that beta power modulation latencies are affected by rhythmicity, and that U-shaped modulation depth predicts pitch perception. The former is consistent with previous findings on the role of beta in temporal prediction (Snyder and Large, 2005; Iversen et al., 2009; Fujioka et al. 2009, 2015, 2012; Cirelli et al., 2014; Morillon and Baillet, 2017). Furthermore, we found that the depth of U-shaped beta power modulation predicts pitch discrimination sensitivity on a trial-by-trial basis. Thus, our data indicate that beta power modulation shape affects sensory predictions, and anticipatorily facilitates perceptual performance. A few previous studies hinted at the role of beta in prediction of pitch. Specifically, beta power was shown to increase *after* unexpected pitch changes (Chang et al., 2016; Franken et al., 2018), to reflect the magnitude of pitch prediction updating (Sedley et al., 2016), and to relate to smaller event-related potential pitch prediction error responses (Chang et al., 2018). However, the lack of behavioural tasks in these studies makes it challenging to link the neural findings with perception. Our finding in the current study that entrained beta power modulation shape prior to a pitch change affects pitch perception adds to previous literature indicating that non-entrained beta power reflects information integration leading to improved perceptual performance across many domains (e.g., Arnal et al., 2015; Herrmann et al., 2016; Kayser et al., 2016; Florin et al., 2017; Pefkou et al., 2017; Spitzer and Haegens, 2017). Note that we found no association between beta desynchronization latency and either pitch discrimination sensitivity or RT on a trial-by-trial basis. It is unclear why rhythmicity affected beta desynchronization latency, but beta modulation depth predicted the discrimination sensitivity at the trial-by-trial level under the Rhythmic condition. Nevertheless, considering that rhythmicity of the sensory input modulates whether the temporal attending mode is rhythmic or not (Nobre and van Ede, 2018), a possible explanation is that the beta desynchronization latency effect reflects the difference between distinct attending modes and beta modulation depth reflects the trial-by-trial neural mechanism of facilitating pitch discrimination under the rhythmic attending mode. In sum, data across studies suggest that for audition, both delta phase and beta power modulation latencies might relate to the prediction of rhythmic temporal regularity; but that delta phase may proactively facilitate perception in the temporal and intensity domains, whereas the U-shaped beta power modulation depth may relate to the spectral domain, including prediction of pitch change and the quality of pitch perception.

Behaviourally, despite the fact that pitch is a fundamental aspect of the perception of sound and critical for both speech and musical processing, we provide novel evidence that rhythmicity improves near-threshold pitch sensitivity. It adds to previous literature indicating that rhythmicity affects sensitivity to deviations in timing and intensity and detecting signals in noise (e.g., Henry and Herrmann, 2014; Hickok et al., 2015). Evidence that rhythmic regularity facilitates detection of large (supra-threshold) pitch changes is inconsistent (Jones et al., 2002; Morillon et al., 2016, but see Bauer et al., 2015), so further research is needed to determine whether near-threshold and supra-threshold pitch discrimination are differentially affected by rhythmic context. In the absence of a predictable rhythmic context, one study found that predictability of a timing delay between isolated cue-target pairs was associated with decreased RT in a pitch discrimination task (Herbst and Obleser, 2017). However, this study did not show any effects on accuracy, and thus it cannot distinguish whether the effects of shortened RT were caused by facilitated perception or simply better motor preparation due to the predictable intervals. The current psychophysical results

further showed that perceptual pitch sensitivity was improved in a rhythmic context. Together our study and that of Herbst and Obleser (2017) suggest that predictable temporal structure in general, whether it arises from a rhythmic context or memory for a time interval, facilitates fine pitch discrimination.

Finally, the present results show that delta-beta phase-amplitude coupling predicts RT but not sensitivity of pitch discrimination, suggesting that cross-frequency coupling reflects auditory-motor interaction. Phase-amplitude coupling is thought to result when the excitatory or inhibitory phase of low-frequency oscillations modulates the power in high-frequency oscillations (Hyafil et al., 2015), such that processing is optimized for rhythmic input (Lakatos et al., 2005; Schroeder and Lakatos, 2009). Only a few studies have reported that delta-beta coupling affects perceptual performance. For example, delta-beta coupling was reported to associate with the accuracy of detecting an auditory temporal delay (Arnal et al., 2015) and comprehending speech (Keitel et al., 2018). In a visual task, delta-beta coupling in primary motor cortex associated with enhanced visual performance (Saleh et al., 2010). In auditory tasks, delta-beta coupling reflects the communication between motor and auditory cortical regions and might modulate perceptual and behavioural selection (Morillon and Baillet, 2017). Our finding is consistent with this idea that delta-beta coupling reflects the efficiency of auditory-motor communication, as shorter RTs would indicate faster information transfer between auditory and motor regions, resulting in faster response selection.

It is an open question as to why we observed that U-shaped beta power modulation depth correlated with pitch discrimination at the left auditory cortex but delta-beta coupling with RT at right auditory cortex. We did not have an a priori hypothesis about lateralization, as the vast majority of previous studies did not examine hemispheric differences. To our knowledge, there are only two previous studies using MEG that looked at hemispheric lateralization. Our lateralization pattern is in line with these previous studies in that they found that the beta effect is localized to the left hemisphere and the delta effect is localized to the right hemisphere (Morillon and Baillet, 2017; Tal et al., 2017). Together, although further investigation is needed, these lateralization findings suggest that left and right auditory cortices associate with different neural entrainment mechanisms and perceptual performances.

The current study focused on neural activities generated from bilateral auditory cortices because they are regarded to be the primary regions for processing pitch in the brain (McDermott, 2018) and are typically reported to be an important source of neural entrainment activities in response to auditory sequences (Fujioka et al., 2012; Morillon and Baillet, 2017). Indeed, most studies investigating auditory neural entrainment activities focus on the neural signal from auditory cortex, either through direct electrophysiological recording, source modeling, or analysis of surface electrodes that predominantly record activity from auditory cortex (e.g., Lakatos et al., 2013; Henry et al., 2014; Morillon and Baillet, 2017; ten Oever et al., 2017). However, neural entrainment activities in response to auditory sequences can also be observed in other cortical regions, including sensorimotor, premotor, supplementary motor and inferior-frontal regions (Besle et al., 2011; Fujioka et al., 2012; Morillon and Baillet, 2017). Examining the activities from those regions is beyond the scope of the current study, given the lack of individual structural scans or sufficient spatial specificity of EEG to reliably extract the neural activities from motor and frontal regions. Nevertheless, we argue that the oscillatory activities from auditory cortex should be most relevant for studying rhythmic facilitation of pitch discrimination. Further studies are needed to examine the perceptual functions of neural entrainment activities beyond auditory cortex.

Many behavioural and neural studies suggest that auditory and motor systems cooperate in processing rhythm (e.g., Phillips-Silver and Trainor, 2005; Chen et al., 2008; Grahn, 2012; Merchant et al., 2015), and beta oscillation is commonly hypothesized as the auditory-motor communication channel (Fujioka et al., 2012; Morillon and Baillet, 2017). Our data suggest delta-beta coupling is also critical for auditory-motor

interactions. It would be interesting for future studies to examine delta-beta coupling in populations with motor deficits, such as Parkinson's patients, who are known to have reduced beta power entrainment to auditory rhythms (te Woerd et al., 2018). Indeed, we have hypothesized that children with developmental coordination disorder will show reduced beta and delta-beta entrainment (Trainor et al., 2018), and others have proposed that interpersonal auditory-motor synchronization (e.g., joint music performance) may involve beta coupling between brains (Novembre et al., 2017).

It is important to note that our Rhythmic condition used the same repetitive isochronous intervals while the Arrhythmic condition used random intervals, and thus the perceptual facilitation effect could be caused by either rhythmicity or by memorizing the predictable fixed single interval or both (Breska and Deouell, 2017; Herbst and Obleser, 2017). Neurally, it has been shown that a predictable fixed single interval without rhythmicity can increase low-frequency phase clustering, so this index might reflect non-oscillatory neural ramping activity (e.g., contingent negative variation) rather than neural oscillation (Breska and Deouell, 2017, but see Obleser et al., 2017). For the current study, we did not aim to eliminate the potential effect of a predictable fixed single interval on perceptual performance, as a fixed interval is inevitably embedded in any isochronous rhythmic sequences. The rhythmic/arrhythmic manipulation was an approach for examining temporal prediction, whether of a rhythmic or fixed interval nature. The important behavioural contribution of the current study is in demonstrating that rhythmic temporal predictability facilitates pitch perception in audition. Future studies are needed to examine whether the effects reported in the current study can be generalized to other forms of temporal predictability, such as cue-target association, hazard rate and repeated intervals (e.g., Breska and Deouell, 2017; Herbst and Obleser, 2017; Nobre and van Ede, 2018). As for delta phase, the current time-frequency neural measurement cannot dissociate possible ramping activities from oscillatory activities. It is possible that the null correlational results between delta phase and behavioural pitch performance were due to confounding ramping neural activities; however, many previous studies have reported an association between delta phase and rhythmic perceptual facilitation, although it remains unclear whether ramping neural activities played a role. In general, separating oscillatory and non-oscillatory neural activities in low-frequency neural oscillations is challenging and needs to be addressed in further careful studies (Doelling et al., 2019).

In a broader theoretical context, the composition of two coupled neural entrainment activities with dissociable functions is consistent with dynamic attending theory. It posits two components: oscillatory temporal expectation and temporal attention (Large and Jones, 1999) in an auditory-motor network (Large et al., 2015). The alignment between these two components enables attention to be anticipatorily deployed for tracking rhythmic sensory sequences and enhancing attention, and therefore perceptual sensitivity, at critical points in time. Our post-hoc speculation is that delta phase might reflect oscillatory temporal expectation and beta power might reflect temporal attention. In particular, our finding that delta phase is affected by rhythmicity but is not related to perceptual pitch enhancement suggests that the primary role of delta oscillations might concern temporal structure prediction rather than facilitating fine spectral perception (i.e., pitch discrimination). Our finding that depth of U-shaped beta power modulation predicts pitch discrimination sensitivity might be explained as beta reflecting enhanced auditory attention at particular time points, where perceptual gain is increased. This speculative framework is consistent with previous studies showing that delta phase entrainment (temporal expectation) is critical for time and intensity tasks. This idea is also consistent with converging evidence that the phase of low-frequency oscillation reflects top-down sensory selection among multiple sensory streams, that the power of high-frequency oscillation implements endogenous perceptual processes or attentional gain, and that the alignment between these two optimizes perceptual performance (Arnal and Giraud, 2012; Henry and Herrmann, 2014; Lakatos et al., 2013, 2016; Morillon and Baillet, 2017; Schroeder

and Lakatos, 2009; Saleh et al., 2010). Additional evidence comes from a study that mathematically modeled MEG recordings in the context of dynamic attending theory, to show that delta oscillations link to temporal expectations (Herrmann et al., 2016). The current study extends this model to beta oscillations, but only shows a single-dissociation with correlational evidence; the differential roles of delta, beta and delta-beta coupling suggested by the present data would be strengthened by further studies showing causal evidence of a triple-dissociation.

The findings of the current study are relevant to speech perception. First, the proposal that the theta phase (4–8 Hz) tracks speech envelope, and nested gamma power (~25–35 Hz) aligns neuronal excitability to acoustic structure for perceiving speech (Giraud and Poeppel, 2012) is similar to our proposal that delta phase reflects temporal prediction and U-shaped beta power modulation depth associates with temporal attention. Second, rhythm facilitates both speech perception (Haegens and Zion Golumbic, 2018) and pitch discrimination (present findings), suggesting beta modulation reflects the "content" of auditory perception. This relationship might also reflect that frequency modulation is crucial for speech recognition (Zeng et al., 2005).

5. Conclusion

We present the novel finding that the temporal regularity of rhythmic sound sequences facilitates perceptual processing of pitch, and that neural oscillatory entrainment activities from auditory cortex, including delta phase, beta power modulation, and delta-beta coupling, are all modulated by rhythmicity. At the same time, trial-by-trial analyses showed that U-shaped beta power modulation depth predicts discrimination sensitivity whereas delta-beta coupling strength predicts reaction time. Future studies should investigate whether temporal predictability in other contexts such as cue-target association, hazard rate, and repeated intervals also enhance pitch perception. With respect to a neural instantiation of dynamic attending theory, our findings suggest a speculative interpretation that delta phase maps onto oscillatory temporal expectations, beta power onto temporal attention, and delta-beta coupling onto the efficiency of auditory-motor communication. Understanding how these neural oscillations work together is critical for uncovering the auditory-motor network and the neural basis of the perception of dynamic auditory inputs such as speech and music.

Appendix A. Supplementary data

Supplementary data to this article can be found online at https://doi.org/10.1016/j.neuroimage.2019.05.007.

References

Arnal, L.H., Doelling, K.B., Poeppel, D., 2015. Delta–beta coupled oscillations underlie temporal prediction accuracy. Cerebr. Cortex 25, 3077–3085.

Arnal, L.H., Giraud, A.L., 2012. Cortical oscillations and sensory predictions. Trends Cognit. Sci. 16, 390–398.

Barr, D.J., Levy, R., Scheepers, C., Tily, H.J., 2013. Random effects structure for confirmatory hypothesis testing: keep it maximal. J. Mem. Lang. 68, 255–278.

Bauer, A.K.R., Bleichner, M.G., Jaeger, M., Thorne, J.D., Debener, S., 2018. Dynamic phase alignment of ongoing auditory cortex oscillations. Neuroimage 167, 396–407.

Bauer, A.K.R., Jaeger, M., Thorne, J.D., Bendixen, A., Debener, S., 2015. The auditory dynamic attending theory revisited: a closer look at the pitch comparison task. Brain Res. 1626, 198–210.

Benjamini, Y., Hochberg, Y., 1995. Controlling the false discovery rate: a practical and powerful approach to multiple testing. J. R. Stat. Soc. B Met 57, 289–300.

Besle, J., Schevon, C.A., Mehta, A.D., Lakatos, P., Goodman, R.R., McKhann, G.M., Emerson, R.G., Schroeder, C.E., 2011. Tuning of the human neocortex to the temporal dynamics of attended events. J. Neurosci. 31, 3176–3185.

Breska, A., Deouell, L.Y., 2017. Neural mechanisms of rhythm-based temporal prediction: delta phase-locking reflects temporal predictability but not rhythmic entrainment. PLoS Biol. 15, e2001665.

Calderone, D.J., Lakatos, P., Butler, P.D., Castellanos, F.X., 2014. Entrainment of neural oscillations as a modifiable substrate of attention. Trends Cognit. Sci. 18, 300–309.

Canolty, R.T., Edwards, E., Dalal, S.S., Soltani, M., Nagarajan, S.S., Kirsch, H.E., Berger, M.S., Barbaro, N.M., Knight, R.T., 2006. High gamma power is phase-locked to theta oscillations in human neocortex. Science 313, 1626–1628.

Chang, A., Bosnyak, D.J., Trainor, L.J., 2016. Unpredicted pitch modulates beta oscillatory power during rhythmic entrainment to a tone sequence. Front. Psychol. 7, 327.

Chang, A., Bosnyak, D.J., Trainor, L.J., 2018. Beta oscillatory power modulation reflects the predictability of pitch change. Cortex 106, 248–260.

Chang, A., Kragness, H.E., Livingstone, S.R., Bosnyak, D.J., Trainor, L.J., 2019. Body sway reflects joint emotional expression in music ensemble performance. Sci. Rep. 9, 205.

Chang, A., Livingstone, S.R., Bosnyak, D.J., Trainor, L.J., 2017. Body sway reflects leadership in joint music performance. P. Natl. Acad. Sci. USA 114, E4134–E4141.

Chen, J.L., Penhune, V.B., Zatorre, R.J., 2008. Listening to musical rhythms recruits motor regions of the brain. Cerebr. Cortex 18, 2844–2854.

Cirelli, L.K., Bosnyak, D., Manning, F.C., Spinelli, C., Marie, C., Fujioka, T., Ghahremani, A., Trainor, L.J., 2014. Beat-induced fluctuations in auditory cortical beta-band activity: using EEG to measure age-related changes. Front. Psychol. 5, 742.

Cirelli, L.K., Trehub, S.E., Trainor, L.J., 2018. Rhythm and melody as social signals for infants. Ann. NY Acad. Sci. 1423, 66–72.

Cohen, M.X., 2014. Analyzing Neural Time Series Data: Theory and Practice. MIT press.

Cousineau, D., 2005. Confidence intervals in within-subject designs: a simpler solution to Loftus and Masson's method. Tutorials Quant. Methods Psychol. 1, 42–45.

Cravo, A.M., Rohenkohl, G., Wyart, V., Nobre, A.C., 2013. Temporal expectation enhances contrast sensitivity by phase entrainment of low-frequency oscillations in visual cortex. J. Neurosci. 33, 4002–4010.

Ding, N., Patel, A.D., Chen, L., Butler, H., Luo, C., Poeppel, D., 2017. Temporal modulations in speech and music. Neurosci. Biobehav. Rev. 81, 181–187.

Doelling, K.B., Assaneo, M.F., Bevilacqua, D., Pesaran, B., Poeppel, D., 2019. An oscillator model better predicts cortical entrainment to music. Proc. Natl. Acad. Sci. 116 (20), 10113–10121.

Florin, E., Vuvan, D., Peretz, I., Baillet, S., 2017. Pre-target neural oscillations predict variability in the detection of small pitch changes. PLoS One 12, e0177836.

Franken, M.K., Eisner, F., Acheson, D.J., McQueen, J.M., Hagoort, P., Schoffelen, J.M., 2018. Self-monitoring in the cerebral cortex: neural responses to small pitch shifts in auditory feedback during speech production. Neuroimage 179, 326–336.

Fujioka, T., Ross, B., Trainor, L.J., 2015. Beta-band oscillations represent auditory beat and its metrical hierarchy in perception and imagery. J. Neurosci. 35, 15187–15198.

Fujioka, T., Trainor, L.J., Large, E.W., Ross, B., 2009. Beta and gamma rhythms in human auditory cortex during musical beat processing. Ann. NY Acad. Sci. 1169, 89–92.

Fujioka, T., Trainor, L.J., Large, E.W., Ross, B., 2012. Internalized timing of isochronous sounds is represented in neuromagnetic beta oscillations. J. Neurosci. 32, 1791–1802.

Giraud, A.L., Poeppel, D., 2012. Cortical oscillations and speech processing: emerging computational principles and operations. Nat. Neurosci. 15, 511–517.

Godey, B., Schwartz, D., De Graaf, J.B., Chauvel, P., Liegeois-Chauvel, C., 2001. Neuromagnetic source localization of auditory evoked fields and intracerebral evoked potentials: a comparison of data in the same patients. Clin. Neurophysiol. 112, 1850–1859.

Grahn, J.A., 2012. Neural mechanisms of rhythm perception: current findings and future perspectives. Top. Cogn. Sci. 4, 585–606.

Haegens, S., Zion Golumbic, E., 2018. Rhythmic facilitation of sensory processing: a critical review. Neurosci. Biobehav. Rev. 86, 150–165.

Henry, M.J., Herrmann, B., Obleser, J., 2014. Entrained neural oscillations in multiple frequency bands comodulate behavior. P. Natl. Acad. Sci. USA 111, 14935–14940.

Henry, M.J., Herrmann, B., 2014. Low-frequency neural oscillations support dynamic attending in temporal context. Timing & Time Percept. 2, 62–86.

Henry, M.J., Obleser, J., 2012. Frequency modulation entrains slow neural oscillations and optimizes human listening behavior. P. Natl. Acad. Sci. USA 109, 20095–20100.

Herbst, S.K., Obleser, J., 2017. Implicit variations of temporal predictability: shaping the neural oscillatory and behavioural response. Neuropsychologia 101, 141–152.

Herrmann, B., Henry, M.J., Haegens, S., Obleser, J., 2016. Temporal expectations and neural amplitude fluctuations in auditory cortex interactively influence perception. Neuroimage 124, 487–497.

Hickok, G., Farahbod, H., Saberi, K., 2015. The rhythm of perception: entrainment to acoustic rhythms induces subsequent perceptual oscillation. Psychol. Sci. 26, 1006–1013.

Hyafil, A., Giraud, A.L., Fontolan, L., Gutkin, B., 2015. Neural cross-frequency coupling: connecting architectures, mechanisms, and functions. Trends Neurosci. 38, 725–740.

Iversen, J.R., Repp, B.H., Patel, A.D., 2009. Top-down control of rhythm perception modulates early auditory responses. Ann. NY Acad. Sci. 1169, 58–73.

Jones, M.R., Moynihan, H., MacKenzie, N., Puente, J., 2002. Temporal aspects of stimulus-driven attending in dynamic arrays. Psychol. Sci. 13, 313–319.

Jung, T.P., Makeig, S., Humphries, C., Lee, T.W., Mckeown, M.J., Iragui, V., Sejnowski, T.J., 2000. Removing electroencephalographic artifacts by blind source separation. Psychophysiology 37, 163–178.

Kayser, S.J., McNair, S.W., Kayser, C., 2016. Prestimulus influences on auditory perception from sensory representations and decision processes. P. Natl. Acad. Sci. USA 113, 4842–4847.

Keitel, A., Gross, J., Kayser, C., 2018. Perceptually relevant speech tracking in auditory and motor cortex reflects distinct linguistic features. PLoS Biol. 16, e2004473.

Kingdom, F.A.A., Prins, N., 2010. Psychophysics: A Practical Introduction. Academic Press.

Lakatos, P., Barczak, A., Neymotin, S.A., McGinnis, T., Ross, D., Javitt, D.C., O'Connell, M.N., 2016. Global dynamics of selective attention and its lapses in primary auditory cortex. Nat. Neurosci. 19, 1707.

Lakatos, P., Musacchia, G., O'Connel, M.N., Falchier, A.Y., Javitt, D.C., Schroeder, C.E., 2013. The spectrotemporal filter mechanism of auditory selective attention. Neuron 77, 750–761.

Lakatos, P., Shah, A.S., Knuth, K.H., Ulbert, I., Karmos, G., Schroeder, C.E., 2005. An oscillatory hierarchy controlling neuronal excitability and stimulus processing in the auditory cortex. J. Neurophysiol. 94, 1904–1911.

Large, E.W., Herrera, J.A., Velasco, M.J., 2015. Neural networks for beat perception in musical rhythm. Front. Syst. Neurosci. 9, 159.

Large, E.W., Jones, M.R., 1999. The dynamics of attending: how people track time-varying events. Psychol. Rev. 106, 119.

Levitt, H., 1971. Transformed up-down methods in psychoacoustics. J. Acoust. Soc. Am. 49, 467–477.

Luck, S.J., Gaspelin, N., 2017. How to get statistically significant effects in any ERP experiment (and why you shouldn't). Psychophysiology 54, 146–157.

McAuley, J.D., Fromboluti, E.K., 2014. Attentional entrainment and perceived event duration. Philos. Trans. R. Soc. Lond. B Biol. Sci. 369, 20130401.

McDermott, J.H., 2018. Audition. In: Stevens' Handbook of Experimental Psychology and Cognitive Neuroscience, fourth ed., vol. 2 Sensation, Perception, and Attntion.

Meijer, D., te Woerd, E., Praamstra, P., 2016. Timing of beta oscillatory synchronization and temporal prediction of upcoming stimuli. Neuroimage 138, 233–241.

Merchant, H., Grahn, J., Trainor, L., Rohrmeier, M., Fitch, W.T., 2015. Finding the beat: a neural perspective across humans and non-human primates. Philos. Trans. R. Soc. Lond. B Biol. Sci. 370, 20140093.

Morillon, B., Baillet, S., 2017. Motor origin of temporal predictions in auditory attention. P. Natl. Acad. Sci. USA 114, E8913–E8921.

Morillon, B., Schroeder, C.E., Wyart, V., Arnal, L.H., 2016. Temporal prediction in lieu of periodic stimulation. J. Neurosci. 36, 2342–2347.

Näätänen, R., Picton, T., 1987. The N1 wave of the human electric and magnetic response to sound: a review and an analysis of the component structure. Psychophysiology 24, 375–425.

Ng, B.S.W., Logothetis, N.K., Kayser, C., 2012a. EEG phase patterns reflect the selectivity of neural firing. Cerebr. Cortex 23, 389–398.

Ng, B.S.W., Schroeder, T., Kayser, C., 2012b. A precluding but not ensuring role of entrained low-frequency oscillations for auditory perception. J. Neurosci. 32, 12268–12276.

Nobre, A.C., van Ede, F., 2018. Anticipated moments: temporal structure in attention. Nat. Rev. Neurosci. 19, 34–48.

Novembre, G., Knoblich, G., Dunne, L., Keller, P.E., 2017. Interpersonal synchrony enhanced through 20 Hz phase-coupled dual brain stimulation. Soc. Cognit. Affect Neurosci. 12, 662–670.

O'Brien, R.G., Kaiser, M.K., 1985. MANOVA method for analyzing repeated measures designs: an extensive primer. Psychol. Bull. 97, 316–333.

Obleser, J., Henry, M.J., Lakatos, P., 2017. What do we talk about when we talk about rhythm? PLoS Biol. 15, e2002794.

Oostenveld, R., Fries, P., Maris, E., Schoffelen, J.M., 2011. FieldTrip: open source software for advanced analysis of MEG, EEG, and invasive electrophysiological data. Comput. Intell. Neurosci. 2011, 156869.

Pefkou, M., Arnal, L.H., Fontolan, L., Giraud, A.L., 2017. θ-Band and β-band neural activity reflects independent syllable tracking and comprehension of time-compressed speech. J. Neurosci. 37, 7930–7938.

Peretz, I., 2016. Neurobiology of congenital amusia. Trends Cognit. Sci. 20, 857–867.

Phillips-Silver, J., Trainor, L.J., 2005. Feeling the beat: movement influences infant rhythm perception. Science 308, 1430.

Prins, N., Kingdom, F.A.A., 2009. Palamedes: matlab routines for analyzing psychophysical data. Available from: http://www.palamedestoolbox.org.

Rohenkohl, G., Cravo, A.M., Wyart, V., Nobre, A.C., 2012. Temporal expectation improves the quality of sensory information. J. Neurosci. 32, 8424–8428.

Saleh, M., Reimer, J., Penn, R., Ojakangas, C.L., Hatsopoulos, N.G., 2010. Fast and slow oscillations in human primary motor cortex predict oncoming behaviorally relevant cues. Neuron 65, 461–471.

Savage, P.E., Brown, S., Sakai, E., Currie, T.E., 2015. Statistical universals reveal the structures and functions of human music. Proc. Natl. Acad. Sci. 112 (29), 8987–8992.

Schroeder, C.E., Lakatos, P., 2009. Low-frequency neuronal oscillations as instruments of sensory selection. Trends Neurosci. 32, 9–18.

Sedley, W., Gander, P.E., Kumar, S., Kovach, C.K., Oya, H., Kawasaki, H., Howard III, M.A., Griffiths, T.G., 2016. Neural signatures of perceptual inference. Elife 5, e11476.

Slotnick, S.D., 2004. Source localization of ERP generators. In: Todd, T.C. (Ed.), Event-Related Potentials: A Methods Handbook. MIT Press, pp. 149–166.

Snyder, J.S., Large, E.W., 2005. Gamma-band activity reflects the metric structure of rhythmic tone sequences. Cogn. Brain Res. 24, 117–126.

Spitzer, B., Haegens, S., 2017. Beyond the status quo: a role for beta oscillations in endogenous content (re) activation. eNeuro 4. ENEURO-0170.

Tal, I., Large, E.W., Rabinovitch, E., Wei, Y., Schroeder, C.E., Poeppel, D., Zion Golumbic, E., 2017. Neural entrainment to the beat: the "missing-pulse" phenomenon. J. Neurosci. 37, 6331–6341.

te Woerd, E.S., Oostenveld, R., de Lange, F.P., Praamstra, P., 2018. Entrainment for attentional selection in Parkinson's disease. Cortex 99, 166–178.

ten Oever, S., Schroeder, C.E., Poeppel, D., van Atteveldt, N., Mehta, A.D., Mégevand, P., Groppe, D.M., Zion Golumbic, E., 2017. Low-frequency cortical oscillations entrain to subthreshold rhythmic auditory stimuli. J. Neurosci. 37, 4903–4912.

Trainor, L.J., Chang, A., Cairney, J., Li, Y.C., 2018. Is auditory perceptual timing a core deficit of developmental coordination disorder? Ann. NY Acad. Sci. 1423, 30–39.

van Driel, J., Cox, R., Cohen, M.X., 2015. Phase-clustering bias in phase–amplitude cross-frequency coupling and its removal. J. Neurosci. Methods 254, 60–72.

Widmann, A., Schröger, E., Maess, B., 2015. Digital filter design for electrophysiological data–a practical approach. J. Neurosci. Methods 250, 34–46.

Zendel, B.R., Lagrois, M.É., Robitaille, N., Peretz, I., 2015. Attending to pitch information inhibits processing of pitch information: the curious case of amusia. J. Neurosci. 35, 3815–3824.

Zeng, F.G., Nie, K., Stickney, G.S., Kong, Y.Y., Vongphoe, M., Bhargave, A., Wei, C., Cao, K., 2005. Speech recognition with amplitude and frequency modulations. P. Natl. Acad. Sci. USA 102, 2293–2298.